Real-Time Incremental Estimation of Retinal Surface Using Laser Aiming Beam

Arpita Routray, Robert A. MacLachlan
The Robotics Institute
Carnegie Mellon University

Joseph N. Martel
Department of Ophthalmology
University of Pittsburgh

Cameron N. Riviere
The Robotics Institute
Carnegie Mellon University

***Abstract*—Vitreoretinal surgery procedures demand high precision and have to be performed with limited visualization and access. Using virtual fixtures in conjunction with robotic surgery has the potential to improve the safety and accuracy of these procedures. A cornerstone of many of these virtual fixtures is reconstruction of the retinal surface with respect to the surgical tool, which is difficult to obtain due to the inadequacy of traditional stereo vision techniques in the intact eye. A structured-light technique applied using an actuated handheld instrument has been proposed to combat this problem, but it only provides a reconstruction at the start of the procedure; it cannot update it as the eye moves during surgery. We propose updating the initial estimate of the retinal plane a single point at a time, by continued detection of a laser aiming beam in each camera frame, as in the initial structured-light approach. This paper presents the technique and demonstrates it via experiment.**

I. Introduction

Vitreoretinal surgery procedures involve manipulating small, delicate structures within the eye and demand high precision. For example, during membrane peeling, the 5-10 μm-thick internal limiting membrane (ILM) has to be removed around macular holes and requires repeated attempts by surgeons over several minutes [1]. Another procedure, retinal vein cannulation, involves drug delivery to retinal vessels less than 100 microns in diameter [2]. In addition to precision requirements, these procedures have to be performed with limited visualization and constrained access, and hence are quite challenging for surgeons. Many robotic platforms have been developed specifically to address these challenges. These include the Preceyes Surgical System [3], the JHU Steady Hand Robot [4], and Micron, an active handheld micromanipulator [5].

Virtual fixtures during robotic vitreoretinal surgery can improve both the safety and accuracy of these procedures [6]. However, an accurate estimate of the position of the retina with respect to the tool tip is a requirement for the success of many of these visual fixtures. Retinal surface estimation is difficult because traditional stereo surface reconstruction methods cannot be used successfully. This is because, during surgery, the optical path involves the cornea, the lens, saline, and also a BIOM (Binocular Indirect OphthalmoMicroscope) lens.

Due to the shortcomings of traditional reconstruction methods in the intact eye, many authors have proposed alternative methods of registering the position of the retina to the surgical tool tip. In [7], the authors use the distance between the tool tip and its shadow in the acquired images to detect proximity, but the method does not provide the exact distance of the tool tip from the retina. A focus-based 3D localization method using the Navarro schematic eye is developed in [8], but the localization error is limited to a few hundred microns.

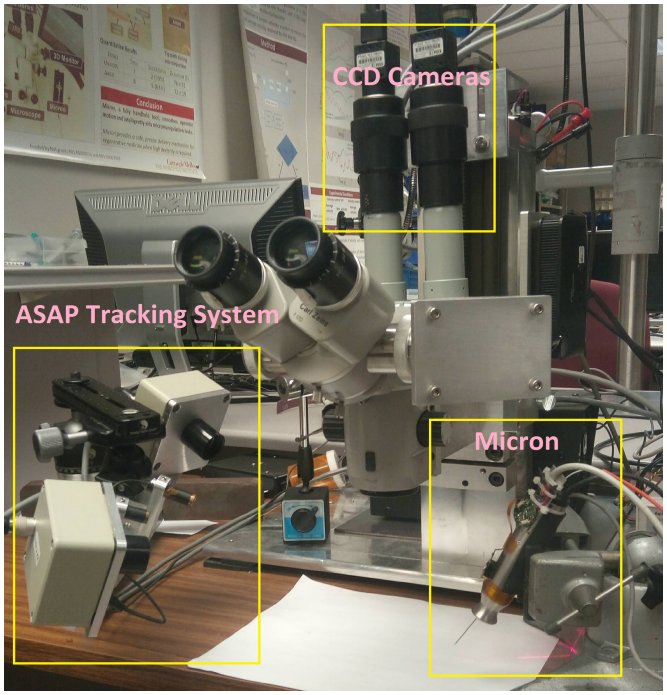

Fig. 1. Micron system setup, showing Micron handheld vitreoretinal surgical instrument, ASAP optical tracker, stereo operating microscope, and cameras.

In all of the above methods, the tool tip is localized using visual feedback. On the other hand, the tool tip of the handheld robot Micron can be tracked at all times using a custom built optical tracking system called Apparatus to Sense Accuracy of Position (ASAP) [9]. Taking advantage of this information, a new method for retinal surface reconstruction was introduced in [10] using structured light applied by a laser aiming beam. This method involves moving the Micron tool tip in a circular trajectory, which is practical only before beginning a surgical procedure, and not during it. Thus, it can only provide an initial estimate of the retinal plane and is not suitable for

978-1-5386-7825-1/19/$31.00 ©2019 IEEE

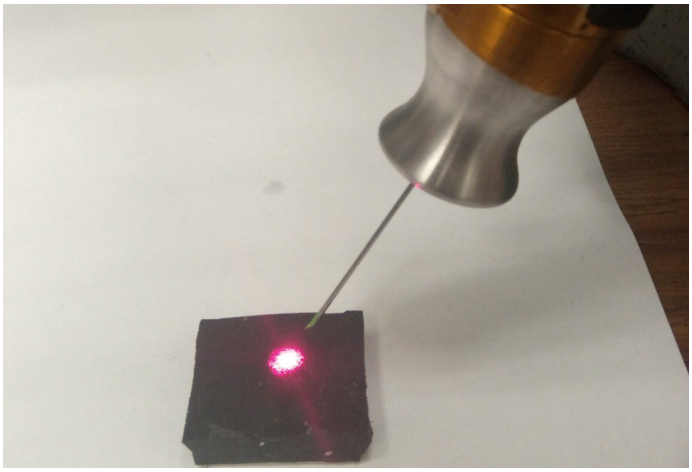

Fig. 2. Laser interfaced with the Micron end-effector.

intraoperative updates.

During vitreoretinal surgery the patient is sedated rather than anesthetized, and movements of the eye are common. To account for movement of the retinal surface, we propose a method that updates the estimate of the retinal plane in real time. At every iteration, the update method computes the position of a single point of the laser aiming beam on the retinal surface in the coordinates of the optical tracking system [9]). However, due to inaccuracies in camera calibration and location of beam center in each frame, these points are noisy. Our method uses these noisy points to update the value of the previous plane estimates. This paper presents the method, and demonstrates the general feasibility wherein a lof updating the retinal plane using a single point per camera frame in an "open-sky" experiment.

II. Methods

Micron is an active handheld robotic instrument for accuracy enhancement that can provide active compensation for the surgeons physiological hand tremor [5] as well as a variety of virtual fixtures [10]. The version of Micron used for this experiment is a six-degree-of-freedom (6DOF) system with the end-effector attached to a prismatic-spherical-spherical Gough Stewart platform that uses piezoelectric linear motors [5]. The end-effector has a cylindrical workspace that is 4mm in diameter and 6mm long with its null position at the centroid of the space. The device has a set of 3 LEDs fixed to the handle, which are optically tracked by ASAP at a sampling rate of 1 kHz. The full 6DOF pose of the handle is computed by triangulating three frequency-multiplexed LEDs mounted on the instrument [9].

The vision system comprises 2 CCD cameras mounted on an operating microscope as shown in Figure 1. All experiments are conducted under the microscope and in full view of the two cameras. The cameras are connected to a desktop PC, which handles image processing.

In order to use the structured-light technique for retinal surface estimation described in [10], a surgical laser is interfaced with Micron, and the end-effector can effectively be used as a laser pointer as shown in Figure 2. The method involves scanning of the micron end-effector in a circular trajectory, resulting in an elliptical laser trajectory on the retinal surface. Geometric analysis of the resulting elliptical pattern gives an estimate of the retinal surface in ASAP coordinates. The method was tested in various conditions and its feasibility was established in a realistic eye model which incorporated optical distortion by lenses.

The human eyeball is a part of a sphere with a diameter of approximately 25 mm. However, the portion of the retina directly visible under the microscope only consists of an area around 4mm wide, which is a small part of this sphere and has relatively lower curvature. Thus, the retinal surface under the microscope can be approximated by a plane and the depth error resulting from this planar assumption is less than 100 μm.

At any point of time t, we first estimate the point at which the laser beam interfaced with micron intersects the retinal surface in 3D ASAP coordinates. Given the noisy triangulated beam points, we then outline a method to update the estimate of a point on the plane and the plane normal. Π_t is used to denote the estimated plane at the instant t. For this study, the initial estimate of the plane at time $t = 0$, Π_0, is assumed as given.

A. Estimation of a Single Point on Retinal Plane

As we are demonstrating the feasibility of our method in open-sky conditions, we use stereo vision to triangulate the position of a single point on the retinal plane. To do so, we first calibrate each camera's 2D image coordinate system to the 3D ASAP coordinate system. To get correspondences between the camera coordinates and ASAP coordinates, the Micron tool tip is detected in each camera and its 3D position

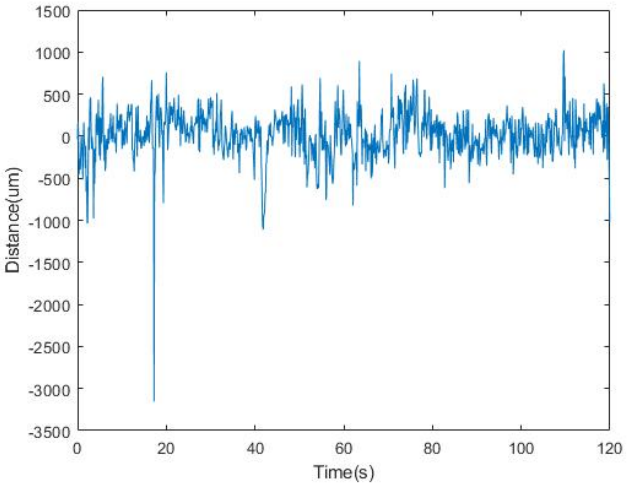

Fig. 3. Distances of the estimated position of the intersection of the laser beam and the retinal surface from the true retinal plane during the surface tracking experiment. The plot demonstrates that the triangulated beam points are noisy, and hence should be filtered.

in ASAP coordinates is recorded simultaneously. Using these correspondences, the projection matrices of both cameras are computed using DLT and RANSAC [6].

In order to optimize the speed of our algorithm, an initial approximation of the center of the laser beam in the left and right camera images, p_{l0}, and p_{r0} is computed using simple thresholding operations. However, as the beam appears diffuse under the microscope, this position may not be the exact point at which the laser beam intersects the retinal surface. We assume that the actual position of the laser beam differs from the initial approximation in the left and right images by constant offsets, ρ_l and ρ_r, respectively. Thus, if p_l and p_r be the actual positions at which the laser beam intersects the retinal surface, we have

$$\begin{aligned} p_l &= p_{l0} + \rho_l \\ p_r &= p_{r0} + \rho_r \end{aligned} \tag{1}$$

For a set of planes Π_i and the corresponding beam locations $p_{l,i}$ and $p_{r,i}$, we define the following terms:

$T(p_{l,i}, p_{r,i})$, the triangulated 3D point using $p_{l,i}$, $p_{r,i}$

d_i, Signed distance between $T(p_{l,i}, p_{r,i})$ and the plane Π_i

$M(d_i)$, Median over all d_i

$\mu_x(|d_i|)$, $x\%$ Trimmed mean over all $|d_i|$

The offsets ρ_l andρ_r are then computed by minimization of the following objective function:

$$F(\rho_l, \rho_r) = 0.5\big|M(d_i)\big| + 0.5\big|\mu_5(|d_i|)\big| + \sqrt{\rho_l^2 + \rho_r^2} \tag{2}$$

Minimization of the first term ensures that the triangulated beam points are distributed evenly above and below the true retinal plane, thus avoiding any offsets during plane estimation. Minimization of the second term reduces the distances of the triangulated beam points from the true retinal plane. The third term is simply used for regularization.

B. Surface Point Update

The triangulated beam points computed in II-A are noisy. In order to filter out high-frequency noise components, we use a moving average filter, and the estimate of a point on the plane is computed as a weighted sum of the previous estimate and the latest filtered beam point. If P_t be the estimate of a point on the plane at time t, then

$$P_t = w_p \sum_{i=t-k_p}^{t} T(p_{l,i}, p_{r,i}) + (1 - w_p) P_{t-1} \tag{3}$$

where the parameters k_p and w_p are the filter window size and the weight corresponding to the latest point update, respectively.

C. Surface Normal Update

An intermediate value of the plane normal, n'_t, is computed by fitting a plane to the last m_n triangulated beam points, such that all points are at least a distance Δ_n away from from each other. The estimate of the plane normal is computed as a weighted sum of the previous estimate and n'_t. If n_t be the estimate of a point on the plane at time t, then

$$n_t = w_n n'_t + (1 - w_n) n_{t-1} \tag{4}$$

where the parameter w_n is the weight corresponding to the latest normal update.

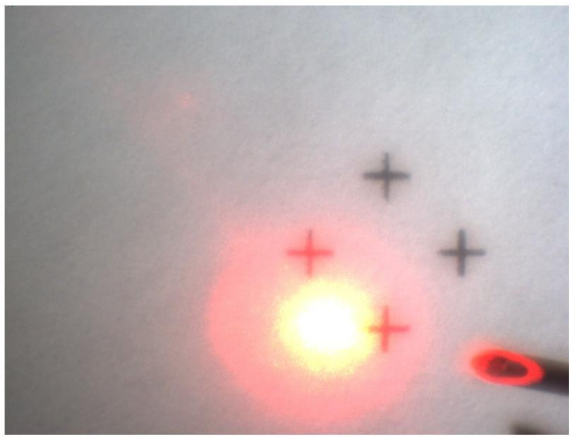

Fig. 4. Fiducials used for estimation of the true plane during the surface tracking experiment.

D. Noisy and Missing Points

If the distance between $T(p_{l,t}, p_{r,t})$ and the estimated plane Π_{t-1} is greater than a threshold Δ_d, or if the laser beam is not detected in the camera images, we set $p_{l,t} = p_{l,t-1}$ and $p_{r,t} = p_{r,t-1}$. P_t and n_t are then computed as usual using (3) and (4). This ensures that the estimated plane is not stagnant during such instances and keeps moving incrementally towards the last position of the triangulated beam point. Hence, once we again get a usable value of $T(p_{l,t}, p_{r,t})$; the plane update resumes with a reduced lag.

E. Experimentation

A separate dataset spanning 100 seconds is used to compute ρ_l andρ_r by optimizing (2). Using this method, we get ρ_l = [1.12, 1.70] pixels and ρ_r = [-2.99, 0.69] pixels. For update of the plane normals, we use the past $m_n = 7$ points, an update weight of $w_n = 0.015$, and a minimum distance between fitted points, $\Delta_n = 50\mu m$. For update of the points on the plane, we use a filter window size of $k_p = 4$ and an update weight of $w_p = 0.2$. The threshold for classifying a point as noise, Δ_d is 5mm. All parameters remain constant throughout the experiment; their values were selected via trial and error.

An initial estimate of the retinal plane is provided at $t = 0$, following which we track changes in this plane over a period of 120 seconds. Over this time period, the plane is rotated and translated manually. Hence, the plane motion is noisy. As shown in Figure 4, four cross-shaped fiducial markers are placed on the surface to be estimated. Ground truth is computed by detecting the centers of the fiducials,

triangulating to obtain their positions in 3D coordinates, and then fitting a plane to these points. This method to obtain ground truth yields reliable estimates of the true retinal plane during the experiment. In frames where the fiducial markers are not visible from the camera due to sudden movements, the ground truth plane is computed by interpolation.

III. Results

Although the optimized offsets ρ_l = [1.12, 1.70] pixels and ρ_r = [-2.99, 0.69] pixels are quite small, the median signed distance $\left|M(d_i)\right|$ and the trimmed mean distance $\mu_5(|d_i|)$, as defined in II-A, reduce by 95.75% and 64.36% in the test dataset.

During the tracking period, we measure the displacement of the updated plane along the ASAP coordinate system's z axis with respect to a stationary point on the initial plane, and find that movement along this axis is compensated by 44.43%. As the plane normal is almost perpendicular to the ASAP system's x and y axes, we do not measure displacement along these other directions. Translations of the estimated plane and the true plane along the z axis over the tracking period is shown in Figure 6. We also measure the angles of the estimated and true plane normals with respect to the ASAP system's x, y, and z axes during this period. These values are plotted over time in Figure 5 and we observe that for the most part, the estimated normal follows the trends of the true plane normal.

IV. Discussion

In this paper, we proposed an algorithm for updating the retinal plane using noisy aiming beam samples, where only one new point is obtained from each incoming camera frame. We demonstrated the general feasibility of the method by tracking a plane in an open-sky experiment using printed fiducial markers as ground truth. We found that our method is able to track changes in the retinal plane in a stable manner, even when the plane is displaced by several millimeters.

Motion of the retinal plane perpendicular to the plane normal does not change its geometrical position in space with respect to the surgical tool tip, and hence cannot be tracked by this algorithm. However, Braun et al. have presented techniques for vision-based intraoperative tracking of retinal vasculature, which can perform this function [11]. Future work will involve combining these algorithms to tracking movements of the retinal surface in six degrees of freedom.

For the surface-tracking experiment conducted in this paper, the parameters used were constant and were selected via trial and error. Although this demonstrated the general feasibility of our method, future work will involve more systematic tuning of these parameters in order to improve the accuracy of the plane update and the lag that is visible in Fig. 5. Since this experiment was conducted open-sky, we were able to use stereo vision to determine the intersection of the laser beam and the retinal surface. Going forward, we plan to investigate finding this point of intersection in an intact eye, which will require alternative means of obtaining ground truth.

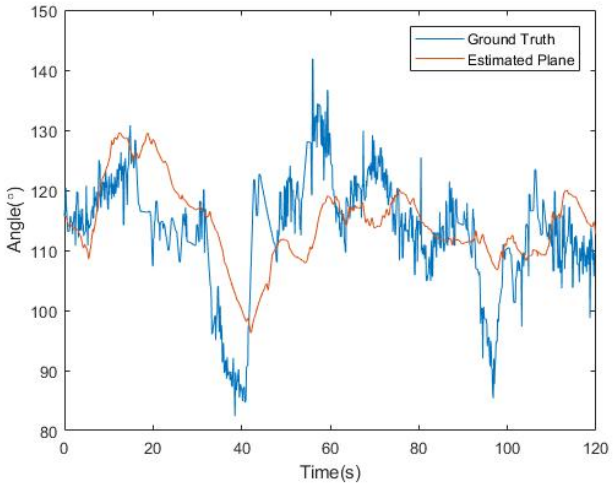

(a) Angle between plane normal and x axis

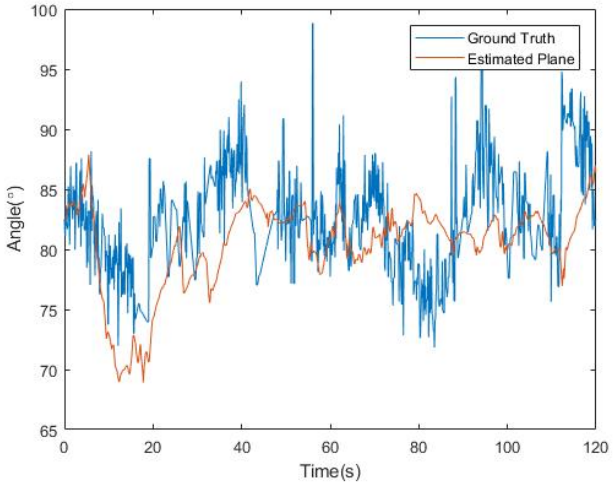

(b) Angle between plane normal and y axis

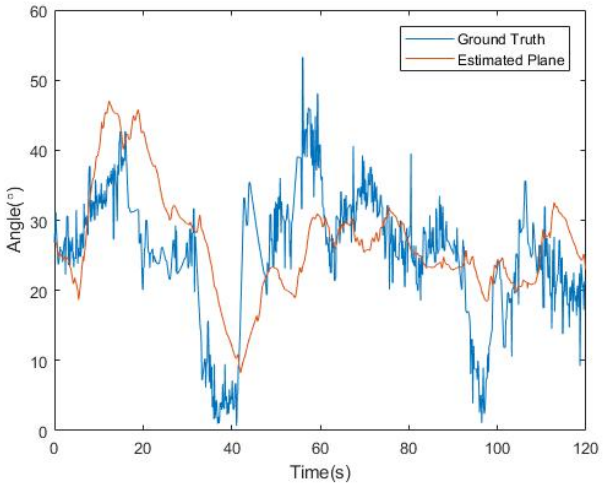

(c) Angle between plane normal and z axis

Fig. 5. Angles of the estimated and true plane normals from the x,y, and z axes during the surface tracking experiment.

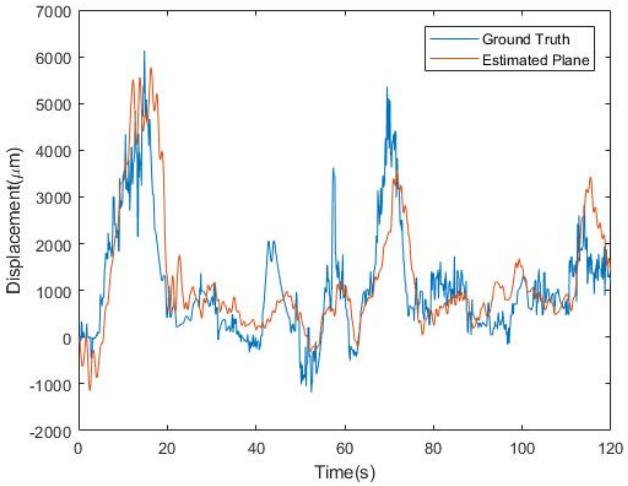

Fig. 6. Plane displacement along z axis over the surface tracking period. The displacement in the z axis is computed with respect to a stationary point on the initial plane.

Application of this technique presupposes the presence of a laser aiming beam in the instrument, which is presently true only of therapeutic laser instruments. However, in principle it is possible to incorporate a laser aiming beam within the intraocular shaft of any type of instrument for any type of intervention. Our group is presently working to incorporate aiming beams into instruments for non-laser retinal operations.

ACKNOWLEDGMENT

Funding provided by U.S. National Institutes of Health (grant no. R01EB000526).

REFERENCES

[1] A. Almony, E. Nudleman, G. K. Shah, K. J. Blinder, D. B. Eliott, R. A. Mittra, and A. Tewari, "Techniques, rationale, and outcomes of internal limiting membrane peeling," *Retina*, vol. 32, no. 5, pp. 877–891, 2012.

[2] K. Kadonosono, S. Yamane, A. Arakawa, M. Inoue, T. Yamakawa, E. Uchio, Y. Yanagi, and S. Amano, "Endovascular cannulation with a microneedle for central retinal vein occlusion," *JAMA Ophthalmology*, vol. 131, no. 6, pp. 783–786, 2013.

[3] T. L. Edwards, K. Xue, H. C. M. Meenink, M. J. Beelen, G. J. L. Naus, M. P. Simunovic, M. Latasiewicz, A. D. Farmery, M. D. de Smet, and R. E. MacLaren, "First-in-human study of the safety and viability of intraocular robotic surgery," *Nature Biomedical Engineering*, vol. 2018, pp. 649–656, 2018.

[4] A. Üneri, M. A. Balicki, J. Handa, P. Gehlbach, R. H. Taylor, and I. Iordachita, "New steady-hand eye robot with micro-force sensing for vitreoretinal surgery," in *Proc. IEEE Int. Conf. Biomedical Robotics and Biomechatronics*, 2010, pp. 814–819.

[5] S. Yang, R. A. MacLachlan, and C. N. Riviere, "Manipulator design and operation of a six-degree-of-freedom handheld tremor-canceling microsurgical instrument," *IEEE/ASME Trans. Mechatron.*, vol. 20, no. 2, pp. 761–772, 2015.

[6] B. C. Becker, R. A. MacLachlan, L. A. Lobes Jr., G. D. Hager, and C. N. Riviere, "Vision-based control of a handheld surgical micromanipulator with virtual fixtures," *IEEE Trans. Robot.*, vol. 29, no. 3, pp. 674–683, 2013.

[7] T. Tayama, Y. Kurose, T. Nitta, K. Harada, Y. Someya, S. Omata, F. Arai, F. Araki, K. Totsuka, T. Ueta *et al.*, "Image processing for autonomous positioning of eye surgery robot in micro-cannulation," *Procedia CIRP*, vol. 65, pp. 105–109, 2017.

[8] C. Bergeles, K. Shamaei, J. J. Abbott, and B. J. Nelson, "Single-camera focus-based localization of intraocular devices," *IEEE Trans. Biomed. Eng.*, vol. 57, no. 8, pp. 2064–2074, 2010.

[9] R. A. MacLachlan and C. N. Riviere, "High-speed microscale optical tracking using digital frequency-domain multiplexing," *IEEE Trans. Instrum. Meas.*, vol. 58, no. 6, pp. 1991–2001, 2009.

[10] S. Yang, J. N. Martel, L. A. Lobes Jr, and C. N. Riviere, "Techniques for robot-aided intraocular surgery using monocular vision," *Int. J. Robotics Research*, vol. 37, no. 8, pp. 931–952, 2018.

[11] D. Braun, S. Yang, J. N. Martel, C. N. Riviere, and B. C. Becker, "EyeSLAM: Real-time simultaneous localization and mapping of retinal vessels during intraocular microsurgery," *International Journal of Medical Robotics and Computer Assisted Surgery*, vol. 14, no. 1, p. e1848, 2018.